Suboptimal Feedback Vibration Control of a Beam with a Proof-Mass Actuator

H. Politansky* and Walter D. Pilkey†
University of Virginia, Charlottesville, Virginia

A clamped-free beam, damped by a proof-mass actuator, is selected for small-scale model research of flexible structures in space. Because of the short length of the actuator, the dynamic behavior of this system is strongly influenced by the constraints on the motion of the proof mass and by the maximum control forces available. An optimal solution is presented, in which a linear programming algorithm is used. Then, by special consideration of the constraints, a simplified suboptimal feedback position control is used, controlling the system by imposing position commands on the proof mass rather than using direct force inputs. The resulting time response closely fits the optimal solution. An adequate response is achieved in the linear and nonlinear regions, even when the proof mass violates its constraints.

Introduction

THE problem of controlling large space structures has received considerable attention in recent years.[1] The proof-mass actuators[2,3] provide a potential means for damping the elastic modes of the structure. They consist of a mass that is free to slide along a finite length track. By use of an electromagnetic force field, the proof mass can be accelerated in either direction along its track, and the resulting reaction force acts on the structure. Because of design limitations[3] the force available is limited, and the track on which the proof mass slides is of a finite length. An electromagnetic force must be applied to avoid violating the end constraints and introducing detrimental nonlinearities.

A prototype structure consisting of a cantilevered beam damped by a proof-mass actuator was designed[4] and is illustrated in Fig. 1. This is a small scale preliminary model for large, flexible space structures. The system contains a proof-mass actuator attached to the free end of the beam. The free endpoint acceleration is measured by a servo-accelerometer. The relative proof-mass position along its track is measured by a proximeter. Heretofore, the primary control approach has been to control the lower frequency vibration modes using a feedback control system designed by a pole-placement technique. For the 25-mm-long actuator, it was found to be difficult to avoid having the proof mass violate its stops, which introduces undamped nonlinear behavior.

One control approach using the so-called "maximum entropy design methodology"[5] was introduced recently. This approach seems to deal with the linear region of the actuator. Another approach is based on limiting performance control theory.[6,7] This method calculates the control force as a function of time for a known system and initial conditions, subject to certain constraints, and minimizes a given performance index. An alternative approach can be obtained by using the dynamic programming method.[8] Numerical results are quite promising, but the computational load with such a control would be heavy and difficult to obtain in real-time systems.

Recent attempts to deal with the proof-mass control problem have either concentrated on the linear region of the actuator or have used computational methods that may be difficult to realize in real-time systems.

A design approach based on optimal control theory is selected in this study. The primary concern here is to obtain the simple feedback control law that works even in the nonlinear region where the proof-mass may violate its stops.

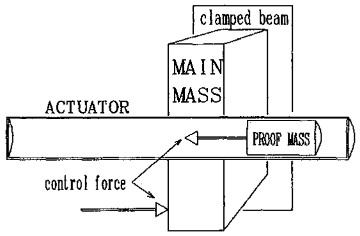

Fig. 1 Clamped-free beam controlled by a proof-mass actuator.

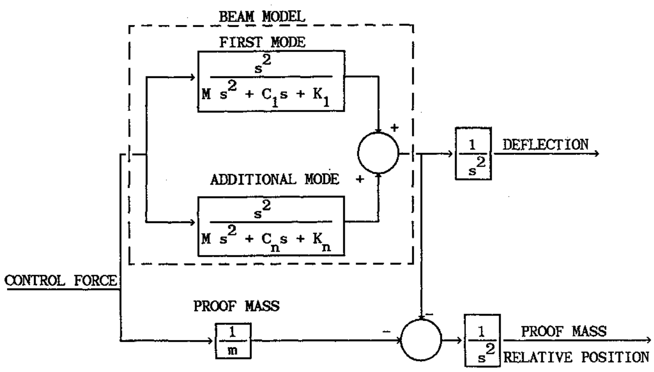

Fig. 2 System model.

A Mathematical Model

A perfect model is rarely obtained for any physical process. One of the most prominent sources of modeling error in large flexible space structures is the deletion of modes in the formation of the design model.[9] The low-frequency modes, which are more accurately known, are retained, and the high-frequency modes are deleted. Here, a simplified one-mode system is used, including the beam's first mode and a perfect proof-mass actuator (with no time delays). Modern

Presented as Paper 87-2323 at the AIAA Guidance, Navigation, and Control Conference, Monterey, CA, Aug. 17–19, 1987; received Jan. 19, 1988; revision received Jan. 16, 1988.

*Visiting Scholar; permanently, Aeronautical and Flight-Control Engineer, Rafael, Ministry of Defense, Haifa, Israel.

†Morse Professor of Mechanical and Aerospace Engineering.

control theory will be used to obtain optimal first-mode performance. The control of the first mode might excite higher modes in the system. The sensitivity of the high-frequency mode will be examined by considering an additional mode as illustrated in Fig. 2. The state equations of the system described in Fig. 2 are

$$\dot{X}_1 = V_1 \tag{1}$$

$$\dot{V}_1 = (-K_1X_1 - C_1V_1 + F_c)/M \tag{2}$$

$$\dot{X}_n = V_n \tag{3}$$

$$\dot{V}_n = (-K_nX_n - C_nV_n + F_c)/M \tag{4}$$

$$\dot{d} = w \tag{5}$$

$$\dot{w} = (K_1X_1 + K_nX_n + C_1V_1 + C_nV_n)/M - F_c(1/m + 2/M) \tag{6}$$

where

X_1, X_n = first and additional mode deflections
V_1, V_n = corresponding velocities
K_1, K_n = equivalent modes stiffness
C_1, C_n = equivalent damping constants
M = equivalent main mass
d, w = proof-mass relative position and velocity
F_c = control force

The system is subjected to the following constraints:

$$|F_c| < F_{\max}, \qquad |d| < d_{\max} \tag{7}$$

We will assume all the modes to be asymptotically stable. Nominal values of the system parameters for the first two modes are given in Table 1.

Table 1 Nominal values of system model parameters

Parameter name	Symbol	Value
Proof mass	m	0.278 kg
Equivalent main mass	M	2.78 kg
First-mode eigenfrequency		6.28 rad/s
Equivalent first-mode stiffness	K_1	109.75 N/m
First-mode damping constant	C_1	≈0.0 kg/s
Second-mode eigenfrequency		≈40.0 rad/s
Equivalent second-mode stiffness	K_n	4314.6 N/m
Second-mode damping constant	C_n	2.2 kg/s
Proof-mass free space	$d_{\max}$	±1.27 cm
Maximum force available	$F_{\max}$	±2.0 N

Unconstrained Optimal Control

The dynamic process is characterized by the system of differential equations:

$$\dot{X} = AX + BU \tag{8}$$

where X is the state vector, U the control vector, and A and B are known matrices. We seek a linear control law of the form

$$U = -K(t)X \tag{9}$$

The matrix $K(t)$ is suitably chosen to minimize the following quadratic performance index

$$J = \frac{1}{2}\int_t^T (X^TQX + U^TRU)\,\mathrm{d}t \tag{10}$$

The matrices Q and R are positive definite and are chosen by the designer. The lower limit on the integral is the present time, the upper limit is the final time, and the time difference is the control interval. The optimal feedback gain is time-varying and depends on the Riccati equation solution[10]:

$$\dot{S} = -A^TS - SA + SBR^{-1}B^TS - Q \tag{11}$$

$$J = \tfrac{1}{2}X^TSX \tag{12}$$

$$K = R^{-1}B^TS \tag{13}$$

We are interested in the steady-state behavior of the process. In this case $\dot{S} = 0$ and satisfies the algebraic Riccati equation (ARE)

$$A^TS + SA - SBR^{-1}B^TS + Q = 0 \tag{14}$$

where

$$K = R^{-1}B^TS \tag{15}$$

When the control law [Eq. (15)] is used to control the process [Eq. (8)], the closed-loop dynamic behavior is given by

$$\dot{X} = A_cX \tag{16}$$

where

$$A_c = A - BK \tag{17}$$

There seems to be two basic types of numerical algorithms for solving the ARE[9]: those that go after the solution directly by iteration and those that proceed indirectly through eigenvalue and eigenvector expansions. In our case the second method is used.

Proof-Mass Control Design Without Consideration of Constraints

Consideration of the first mode in the system shown in Fig. 2 results in the following state equation:

$$\dot{X} = AX + BF_c \tag{18}$$

where

$$\dot{X}^T = [X_1V_1dw] \tag{19}$$

For the nominal values given in Table 1

$$A = \begin{bmatrix} 0 & 1 & 0 & 0 \\ -39.48 & 0 & 0 & 0 \\ 0 & 0 & 0 & 1 \\ 39.48 & 0 & 0 & 0 \end{bmatrix}, \qquad B = \begin{bmatrix} 0 \\ 0.36 \\ 0 \\ -3.96 \end{bmatrix} \tag{20}$$

The first mode eigenvalues are $\pm 6.28i$.

To obtain a damped, closed-loop, first-mode frequency of about 15 rad/s, the following performance index was chosen:

$$J = \int_0^\infty (X_1^2 + 0.001d^2 + 0.000001F_c^2)\,\mathrm{d}t \tag{21}$$

The resulting feedback gain matrix is

$$K = [928.54, -57.65, -31.62, -12.86] \tag{22}$$

The first-mode closed-loop eigenvalues are $-13.16 \pm 14.46i$. The actuator closed-loop eigenvalues are $-1.99 \pm 2.79i$.

The time response for $X_1(0) = 1$ mm is given in Fig. 3. The control system damps the elastic mode within less than one cycle. Increasing the initial condition to $X_1(0) = 1$ cm results in impacting the stops. In such a case, elastic impacts between the proof mass and the end stops are assumed. The velocity changes for elastic impacts are

$$dw = -2w \tag{23}$$

$$dV_1 = 2wm/(M+m) \tag{24}$$

The time response for an impact situation is shown in Fig. 4. The elastic impacts have caused undamped behavior. A possible way to deal with the impacts is to assume plastic impacts in the stops. An alternative method will be discussed later.

Optimal Control Considering Constraints Via Linear Programming

Any suboptimal solution should be compared to the optimal solution. Through the use of a linear programming method,[11] the optimal control can be determined such that an objective function is minimized while the constraints are satisfied. The state of the system is defined at discrete times, and the control forces are assumed to be pulses of constant amplitude across the time intervals. The discrete time representation of the system[12] is given by

$$X_{k+1} = ATX_k + BTU_k \tag{25}$$

where

$$AT = e^{A\,\mathrm{D}t} \tag{26}$$

$$\mathrm{D}t = t_{k+1} - t_k \tag{27}$$

The matrix e^G, for a given square matrix G, is evaluated by

$$e^G = I + \frac{G^1}{1!} + \frac{G^2}{2!} + \frac{G^3}{3!} + \cdots \tag{28}$$

Unbounded control will never appear in practice. The control input will assume to be bounded by

$$U_{\min} \le U_k \le U_{\max} \tag{29}$$

The linear programming method is defined such that positive variables are computed. Normally this restriction is removed by defining each variable as the difference of two new positive unknown variables.[6,7] This approach can be avoided by defining

$$UP_k = U_k - U_{\min} \tag{30}$$

so that all UP_k have positive values.

By using Eqs. (25) and (30), any state variable at any time t_k can be expressed as a function of the initial condition and the input control vector:

$$UH_k^T(m \cdot k) = [UP_1^T(m) \quad UP_2^T(m) \quad \ldots \quad UP_k^T(m)] \tag{31}$$

to satisfy the equalities

$$X_k(n) = B_k(n, m \cdot k)UH_k(m \cdot k) + AT(n,n)^k X_1(n) + C_1(n) \tag{32}$$

where n is the number of state variables; m is the number of controllers; and k is the number of intermediate time steps.

Equations (30) and (32) are used to set up the linear programming tableau[11] as follows:

1) Inequalities due to control constraints for *all* the controllers between the first and final time step [use Eq. (30)]:

$$UH_k \le U_{\max} - U_{\min} \tag{33}$$

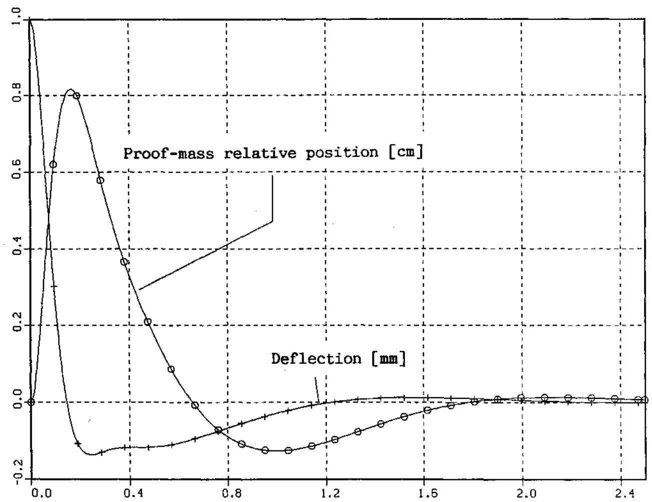

Fig. 3 Linear time response.

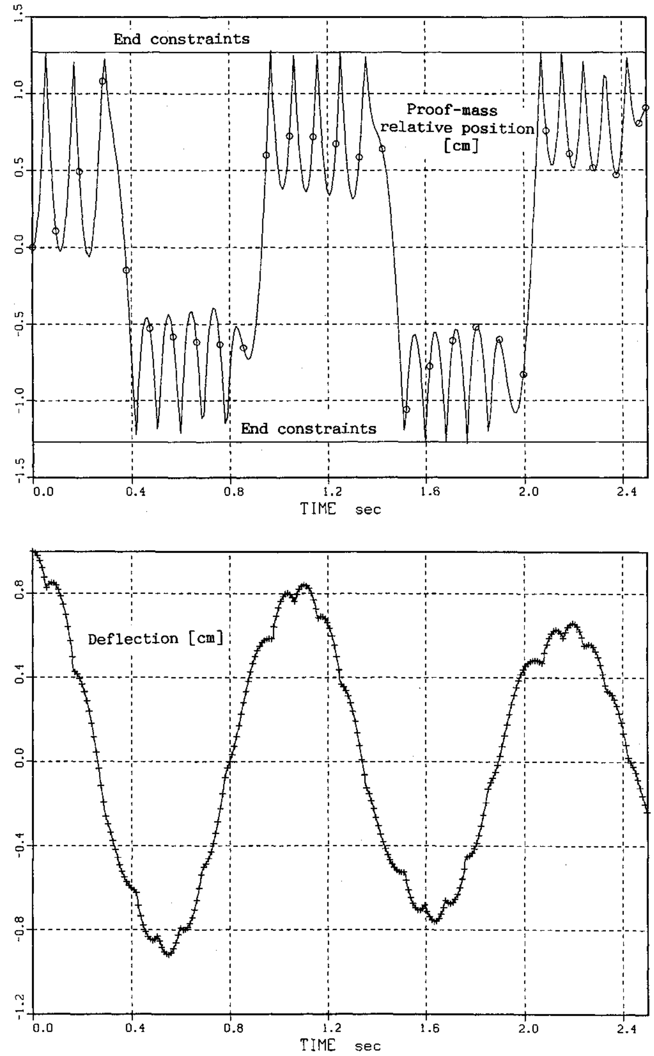

Fig. 4 Nonlinear time response.

2) Inequalities caused by *some* of the state variables that are constrained between the first and the final time steps [use Eq. (32)]:

$$X_k \le X_{\max} \tag{34}$$

$$X_k \le X_{\min} \tag{35}$$

3) Equalities caused by *some* of the state variables for which final values are specified by a given vector $\boldsymbol{X}_{\text{final}}$:

$$X_f = X_{\text{final}} \tag{36}$$

where f is the number of final time steps.

4) Inequalities caused by *some* of the state variables for which final values are to be minimized (not the variable for which the final values are specified above):

$$\boldsymbol{X}_f \le \boldsymbol{X}_b \tag{37}$$

$$\boldsymbol{X}_f \ge -\boldsymbol{X}_b \tag{38}$$

where $\boldsymbol{X}_b$ is a positive unknown vector that bounds the final state. The linear programming task is to find a solution such that the given constraints are satisfied while the objective function is minimized:

$$Z = \boldsymbol{K}_b \boldsymbol{X}_b \tag{39}$$

where $\boldsymbol{K}_b$ is a positive weighting vector.

For a controllable system there are a minimum finite number of time steps $k_{\min}$, in which a zero value for the objective function can be achieved.

For $k < k_{\min}$ we get $Z > 0$, and the solution is a function of $\boldsymbol{K}_b$.

For $k = k_{\min}$ we get $Z = 0$ for any $\boldsymbol{K}_b$. That is the minimum time solution.

For $k > k_{\min}$ we get $Z = 0$, and the solution is not unique. In this case, the minimum time solution is one possible solution.

The algorithm previously described was performed using the simplex method algorithm.[13] A time step size of 0.025 s is selected for our proof-mass system. The minimum time solution for an initial condition $X_1(0) = 1$ cm is presented in Fig. 5. Zero values for all of the state variables are achieved within 2.425 s. The resulting control forces have a complex bang-bang behavior (not shown in Fig. 5). But the proof-mass motion along its finite length track is rather simple. This kind of motion can be implemented by using a direct position control, which will be considered next.

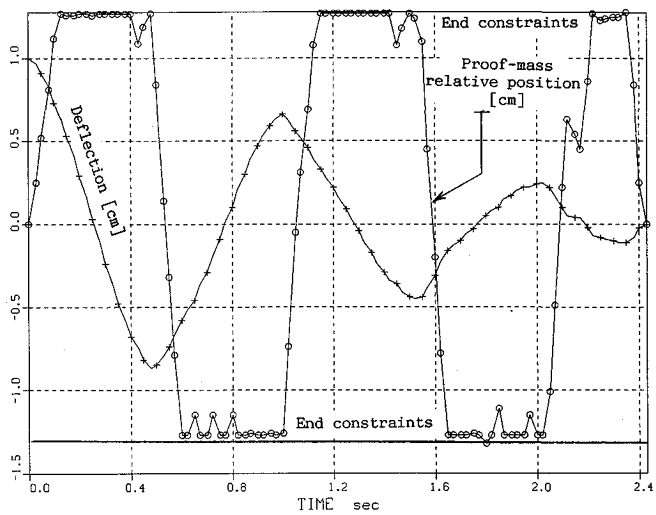

Fig. 5 Minimum time solution.

Suboptimal Control Considering Constraints

The minimum time solution obtained previously implies that a simple controller can be accomplished by controlling the relative position of the proof mass along its track rather than determining direct control force commands. We expand the system by combining it with a position loop, as indicated by the dashed lines in Fig. 6. All of the state variables are assumed to be perfectly known or observed:

- d_c = desired proof-mass relative position
- d = actual position of the proof mass
- a = system acceleration
- K_m, K_p = accelerometer and proximeter gains
- A_1, A_2 = position loop feedback gains

The objective of the accelerometer loop is to feed on force commands because of structure accelerations. The goal of the proximeter loop is to keep the proof mass near its desired relative position. For $K_m = K_p = 1$, $K_m = m$, and considering the first mode in the beam model, the state equations of the system are

$$\dot{X}_1 = \dot{V}_1 \tag{40}$$

$$\dot{V}_1 = (-K_1 X_1 - C_1 V_1 + A_1 md + A_2 mw - A_1 md_c)/(M + m) \tag{41}$$

$$\dot{d} = \omega \tag{42}$$

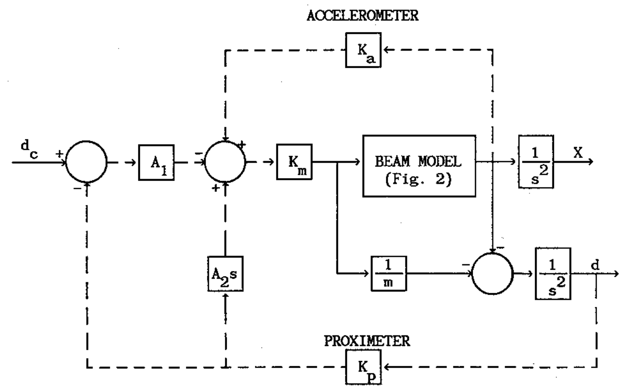

Fig. 6 Position-controlled system.

$$\dot{w} = -A_1 d - A_2 w + A_1 d_2 \tag{43}$$

The system constraints are

$$|F_c| < F_{\max}, \qquad |d| < d_{\max} \tag{44}$$

where

$$F_c = [-a + A_1(d_c - d) + A_2 w]m \tag{45}$$

Because of the accelerometer feedback a_s, the proof-mass relative position d/d_c is insulated from the outside system in the open-loop sense. Its closed-loop dynamics is determined by the proximeter feedback. The resulting transfer function d/d_c is

$$d/d_c = A_1/(s^2 + A_2 s + A_1) \tag{46}$$

We would like Eq. (46) to be critically damped where

$$A_1 = F_{\max}/(m d_{\max}) \tag{47}$$

$$A_2 = 2\sqrt{A_1} \tag{48}$$

Now, by limiting

$$|d_c| < d_{\max} \tag{49}$$

and for

$$a \ll F_{\max}/m \tag{50}$$

the system will not exceed the given constraints [Eq. (44)].

Introducing a position loop into the system and choosing its gains properly make it possible to obtain a system where only the loop's input is constrained. For a general performance index of the form

$$J = \frac{1}{2}\int_t^T L\, dt \tag{51}$$

the optimal control can be treated through Hamilton's principle.[8] The Hamiltonian is defined by

$$H = L + p^T X \tag{52}$$

where p is the co-state vector.

For the case of constrained input, Pontryagin[8] states, "the Hamiltonian must be minimized over all admissible control for optimal values of the state and costate." In the case under consideration, the Hamiltonian is a quadratic function of a single control input, and there is only one location where the Hamiltonian is minimized. The control in this point will be denoted in our case as d_{opt}. Pontryagin's minimum principle leads in this case to the following optimal solution

$$d_c = \begin{bmatrix} d_{max} & \text{for} & d_c > & d_{max} \\ d_{opt} & \text{for} & |d_c| \leq & d_{max} \\ -d_{max} & \text{for} & d_c < & -d_{max} \end{bmatrix} \tag{53}$$

For the chosen gains [Eqs. (47) and (48)] and for the system parameters given in Table 1,

$$A = \begin{bmatrix} 0.00 & 1.00 & 0.00 & 0.00 \\ -35.89 & 0.00 & 48.09 & 4.18 \\ 0.00 & 0.00 & 0.00 & 1.00 \\ 0.00 & 0.00 & -529.00 & -46.00 \end{bmatrix} B = \begin{bmatrix} 0.00 \\ -48.09 \\ 0.00 \\ 529.00 \end{bmatrix} \tag{54}$$

The open-loop eigenvalues are

$$-23.0, \; -23.0, \; \pm 5.99i \tag{55}$$

The following performance index is chosen as

$$J = \int_0^\infty (X_1^2 + \mu d_c^2)\, dt \tag{56}$$

The parameter μ will determine the closed-loop speed of response. For $\mu = 0.001$, the closed-loop eigenvalues are

$$-32.29 \pm 23.37i, \qquad -2.03 \pm 2.80i \tag{57}$$

and the resulting feedback gain matrix is

$$K = [-27.04 \quad 2.74 \quad 0.00 \quad 0.29] \tag{58}$$

The time response for an initial condition $X_1(0) = 1$ cm is given in Fig. 7. Two regions are identified in the optimal solution [Eq. (53)]. For the first 3 s, the optimal input is on the boundaries ($\pm d_{max}$). The proof mass is moving as in the minimum time solution, and the time response closely fits the response shown in Fig. 5.

Sensitivity to High-Frequency Modes

The expected second-mode frequency in our system is about 40 rad/s. It is not far from the closed-loop eigenvalues obtained in Eq. (57). Care must be taken to avoid cross coupling between them. By introducing the additional mode in Fig. 2 to the system with the position loop described in Fig. 6, the following state equations are obtained:

$$\dot{X}_1 = V_1 \tag{59}$$

$$\dot{V}_1 = [-K_1(1 + m/M)X_1 + K_n(m/M)X_n + C_n(m/M)V_n + A_1 md + A_2 mw - A_1 md_c]/(M + 2m) \tag{60}$$

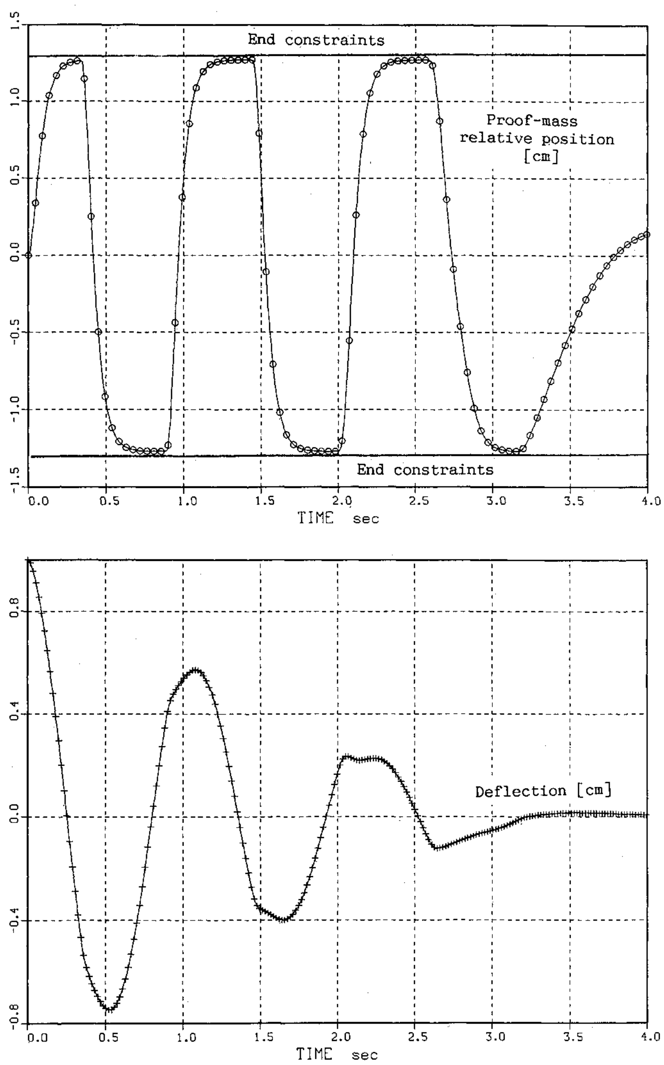

Fig. 7 Closed-loop time response with position control.

$$\dot{X}_n = V_n \tag{61}$$

$$\dot{V}_n = [K_1(m/M)X_1 - K_n(1 + m/M)X_n + C_n(m/M)V_n + A_1 md + A_2 mw - A_1 md_c]/(M + 2m) \tag{62}$$

$$\dot{d} = w \tag{63}$$

$$\dot{w} = -A_1 d - A_2 w + A_1 d_c \tag{64}$$

In matrix notation, the state equation is

$$\dot{X} = AX + Bd_c \tag{65}$$

where

$$X^T = [X_1 \; V_1 \; X_n \; V_n \; dw] \tag{66}$$

For the nominal values given in Table 1 and for A_1 and A_2 chosen as in Eqs. (47) and (48),

$$A = \begin{bmatrix} 0.00 & 1.00 & 0.00 & 0.00 & 0.00 & 0.00 \\ -36.19 & 0.00 & 129.33 & 0.07 & 44.08 & 3.83 \\ 0.00 & 0.00 & 0.00 & 1.00 & 0.00 & 0.00 \\ 3.29 & 0.00 & -1422.68 & -0.73 & 44.08 & 3.38 \\ 0.00 & 0.00 & 0.00 & 0.00 & 0.00 & 1.00 \\ 0.00 & 0.00 & 0.00 & 0.00 & -529.00 & -46.00 \end{bmatrix} \tag{67}$$

$$B^T = [0.00 \quad -44.08 \quad 0.00 \quad -44.08 \quad 0.00 \quad 529.00] \quad (68)$$

The system open-loop eigenvalues are

$$-23, \quad -23, \quad \pm 5.99i, \quad -0.36 \pm 37.72i \quad (69)$$

An attempt to control this second-order system by using the feedback gain matrix [Eq. (58)], obtained for a single-mode model, results in an unstable closed-loop system, as shown in Fig. 8. To avoid this instability, the second mode should be included in the control design. Then, check the sensitivity to the higher modes deleted from the model and hope for the best. This method requires additional information and measurements that might not be available. An alternative approach is to reduce the bandwidth of the closed-loop system up to a point where the control of the low-frequency modes, which are more accurately known, will not excite the expected high-frequency modes. The designer should not attempt to alter the dynamic behavior of the open-loop process more than is required[14] because of the uncertainty of the high-frequency dynamics of the process.

Another reason for limiting the bandwidth is the sensitivity to noise. If the input to the system contains a good deal of noise, it might be desirable to reduce the bandwidth to prevent the system from becoming excessively agitated by following the noise.

In Table 2 we calculate the optimal control for a first-order system as a function of the control effort parameter μ where the performance index is

$$J = \int_0^\infty (X_1^2 + \mu d_c^2)\, dt \quad (70)$$

The feedback control

$$d_c = -K_x X_1 - K_v V_1 - K_d d - K_w w \quad (71)$$

is obtained and the resulting closed-loop eigenvalues of one-mode and two-mode systems are calculated. Increasing μ results in reducing the feedback gains. We have selected the working point marked in Table 2 to obtain a closed-loop bandwidth that is below the expected eigenfrequency of the second mode and does not excite it. The time response of the system for the selected control is given in Fig. 9. The stability of the closed-loop system to the additional mode frequency is examined in Fig. 10. Additional eigenfrequencies in the range of 1–3.75 Hz will be excited ($\zeta < 0$) by the control of the first-mode frequencies. The expected second-mode frequency is about 6 Hz, and higher eigenfrequencies are far above the control system bandwidth and will probably not be affected by it.

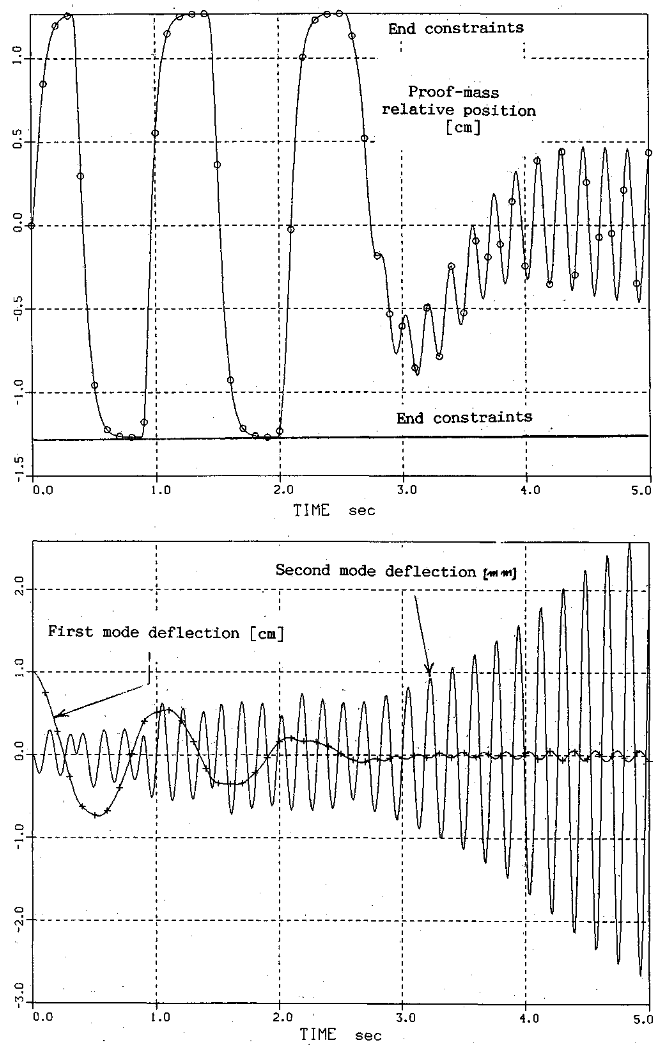

Fig. 8 Effect of the second mode for a high-bandwidth, closed-loop system.

Table 2 Eigenvalues of the closed-loop system as a function of the control effort parameter μ [Eqs. (70) and (71)]

Effort, μ	Feedback gains K_x	K_v	K_w	One-mode system eigenvalues	Two-mode system eigenvalues
0.001	−27.04	2.74	0.29	$-32.29 \pm 23.37i$ $-2.03 \pm 2.80i$	$-38.01 \pm 17.26i$ $-2.33 \pm 2.69i$ $+0.66 \pm 34.93i$
0.005	−10.64	1.55	0.16	$-25.89 \pm 12.78i$ $-2.11 \pm 4.28i$	$-28.63 \pm 6.89i$ $-2.38 \pm 4.35i$ $-0.51 \pm 35.59i$
0.01	−7.05	1.18	0.12	$-24.54 \pm 9.42i$ $-1.88 \pm 4.89i$	$-26.33 \pm 3.89i$ $-2.06 \pm 5.00i$ $-0.70 \pm 36.05i$
0.05	−2.73	0.59	0.06	$-23.31 \pm 4.35i$ $-1.07 \pm 5.71i$	$-29.91 - 18.95$ $-1.11 \pm 5.81i$ $-0.69 \pm 36.90i$
	⇑ selected gains				

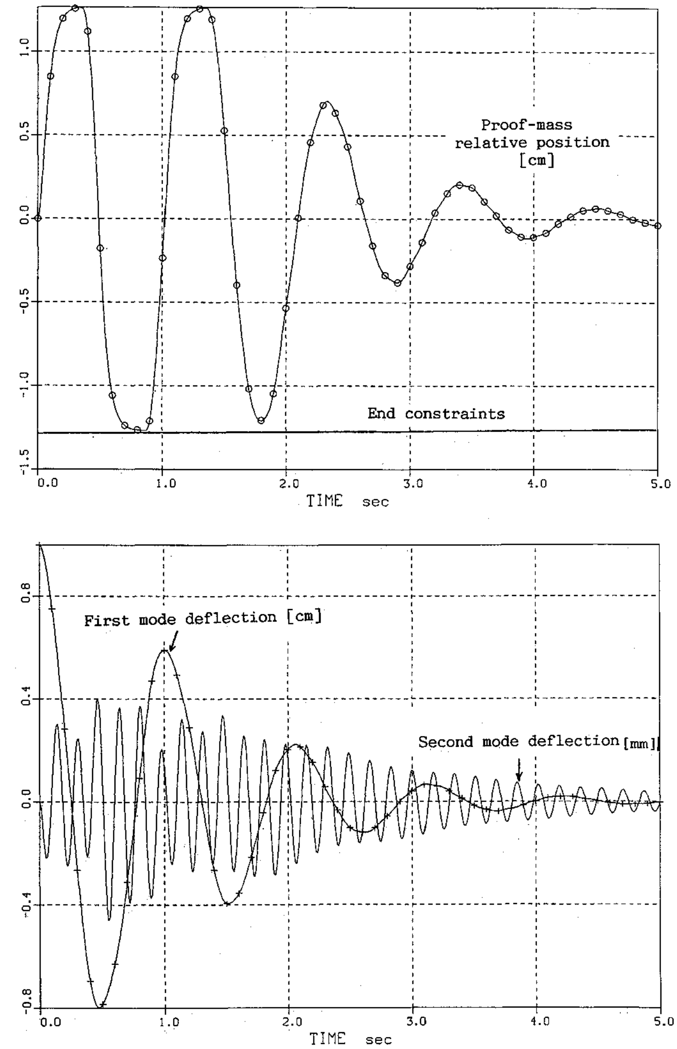

Fig. 9 Effect of the second mode for a low-bandwidth, closed-loop system.

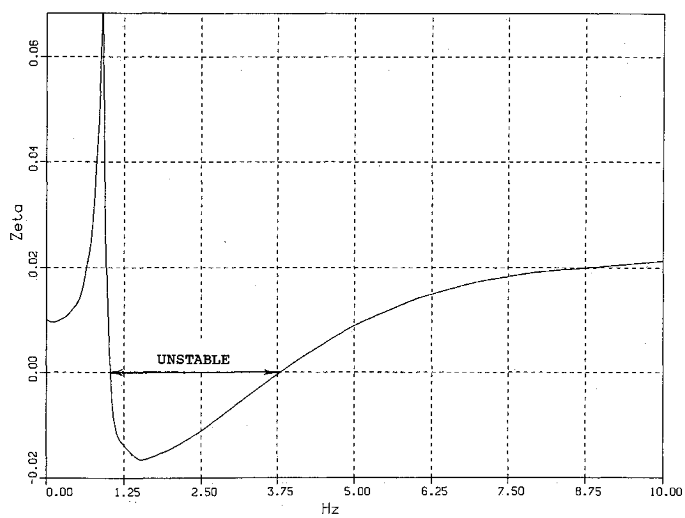

Fig. 10 Effect of the additional mode frequency on the stability of the closed-loop system.

Conclusion

A combined optimal/classical design approach for controlling the vibration of a clamped-free beam by a proof-mass actuator is presented. For short-span actuators, the dynamic behavior of the proof-mass system is dominated by the constraints on the motion of the proof mass and by the maximum control forces available. All recent attempts to deal with this control problem have either concentrated in linear regions, where the proof mass does not violate the end constraint or have used mathematical programming methods, including consideration of the constraints, but leading to a system that may be difficult to carry out in real time.

In the present work, a minimum time solution is obtained by use of a linear programming method. Then, by special consideration of the constraints and the effects of the residual higher modes in the system, a simplified suboptimal feedback position control is utilized to obtain an optimal low-frequency performance and bounds on the high-frequency modes. Adequate results are obtained for the linear and nonlinear regions, even when the proof mass violates the constraints.

Acknowledgment

This work was supported by the Air Force Office of Scientific Research, Washington, D.C.

References

[1]Nurre, G. S., Ryan, R. S., Scofield, H. N., and Sims, J. L., "Dynamics and Control of Large Space Structures," *Journal of Guidance, Control, and Dynamics*, Vol. 7, Sept.–Oct. 1984, pp. 514–526.

[2]Meirovitch, L., "A Computational Approach to the Control of Large-Order Structures," NASA CP-2258, May 1982.

[3]Zimmerman, D. C., Inman, D. J., and Horner, G. C., "Dynamic Characterization and Microprocessor Control of the NASA/UVA Proof-Mass Actuator," AIAA Paper 84-1077, May 1984.

[4]Mallette, M. F., "Theory and Application of Linear Servo Dampers for Large Scale Space Structures," Ph.D. Dissertation, School of Engineering and Applied Science, Univ. of Virginia, Charlottesville, VA, May 1986.

[5]Gruzen, A. and Vander Velde, W. E., "Robust Reduced-Order Control of Flexible Structures Using the Optimal Projection/Maximum Entropy Design Methodology," AIAA Guidance, Navigation and Control Conference, Williamsburg, VA, Aug. 1986.

[6]Robertson, B. P. and Pilkey, W. D., "Limiting Performance for the Control of Large Vibrating Structures by a Modal Approach," *International Journal of Analytical and Experimental Model Analysis*, 1987.

[7]Haviland, J. K., Lim, T. W., Pilkey, W. D., and Politansky, H., "The Control of Linear Dampers for Large Space Structures," AIAA Guidance, Navigation and Control Conference, Monterey, CA, Aug. 1987.

[8]Lewis, F. L., *Optimal Control*, Wiley, New York, 1986.

[9]Hefner, R. D. and Mingori, D. L., "Robust Controller Design Using Frequency Domain Constraints," *Journal of Guidance and Control*, Vol. 10, March–April 1987, pp. 158–165.

[10]Bryson, A. E., Jr. and Ho, Y. C., *Applied Optimal Control*, Blaisdell, Waltham, MA, 1969.

[11]Kolman, B. and Beck, R. E., *Elementary Linear Programming with Applications*, Academic, New York, 1980.

[12]D'Azzo, J. J. and Houpis, C. H., *Linear Control System Analysis and Design-Conventional and Modern*, McGraw-Hill, New York, 1981.

[13]Press, W. H., Flannery, B. P., Teukolsky, S. A., and Vetterling, W. T., *Numerical Recipes: The Art of Scientific Computing*, Cambridge Univ. Press, New York, 1987.

[14]Friedland, B., *Control System Design: An Introduction to State-Space Methods*, McGraw-Hill, New York, 1986.

[15]Von Flotow, A. H. and Schafer, B., "Wave-Absorbing Controllers for a Flexible Beam," *Journal of Guidance, Control, and Dynamics*, Vol. 9, Nov.–Dec. 1986, pp. 673–680.